ISSN 1674-1056
http://cpb.iphy.ac.cn
http://iopscience.iop.org/cpb
中国物理 B
Chinese Physics
中国物理
Chinese Physics B

Effects of proton irradiations at different incident angles on InAlAs/InGaAs InP-based HEMTs

Shu-Xiang Sun(孙树祥), Zhi-Chao Wei(魏志超), Peng-Hui Xia(夏鹏辉), Wen-Bin Wang(王文斌), Zhi-Yong Duan(段智勇), Yu-Xiao Li(李玉晓), Ying-Hui Zhong(钟英辉), Peng Ding(丁芃), Zhi Jin(金智)
Citation: Chin. Phys. B . 2018, 27(2): 028502. **doi:** 10.1088/1674-1056/27/2/028502

Journal homepage: http://cpb.iphy.ac.cn; http://iopscience.iop.org/cpb

What follows is a list of articles you may be interested in

Detailed study of NBTI characterization in 40-nm CMOS process using comprehensive models

Yan Zeng(曾严), Xiao-Jin Li(李小进), Jian Qing(卿健), Ya-Bin Sun(孙亚宾), Yan-Ling Shi(石艳玲), Ao Guo(郭奥), Shao-Jian Hu(胡少坚)
Chin. Phys. B . 2017, 26(10): 108503. **doi:** 10.1088/1674-1056/26/10/108503

Improved high-frequency equivalent circuit model based on distributed effects for SiGe HBTs with CBE layout

Ya-Bin Sun(孙亚宾), Xiao-Jin Li(李小进), Jin-Zhong Zhang(张金中), Yan-Ling Shi(石艳玲)
Chin. Phys. B . 2017, 26(9): 098502. **doi:** 10.1088/1674-1056/26/9/098502

Impact of energy straggle on proton-induced single event upset test in a 65-nm SRAM cell

Bing Ye(叶兵), Jie Liu(刘杰), Tie-Shan Wang(王铁山), Tian-Qi Liu(刘天奇), Jie Luo(罗捷), Bin Wang(王斌), Ya-Nan Yin(殷亚楠), Qing-Gang Ji(姬庆刚), Pei-Pei Hu(胡培培), You-Mei Sun(孙友梅), Ming-Dong Hou(侯明东)
Chin. Phys. B . 2017, 26(8): 088501. **doi:** 10.1088/1674-1056/26/8/088501

An optimized fitting function with least square approximation inInAs/AlSb HFET small-signal model for characterizingthe frequency dependency of impact ionization effect

He Guan(关赫), Hui Guo(郭辉)
Chin. Phys. B . 2017, 26(5): 058501. **doi:** 10.1088/1674-1056/26/5/058501

Effect of ionizing radiation on dual 8-bit analog-to-digital converters (AD9058) with various dose rates and bias conditions

Li Xing-Ji, Liu Chao-Ming, Sun Zhong-Liang, Xiao Li-Yi, He Shi-Yu
Chin. Phys. B . 2013, 22(9): 098501. **doi:** 10.1088/1674-1056/22/9/098501

Effects of proton irradiation at different incident angles on InAlAs/InGaAs InP-based HEMTs*

Shu-Xiang Sun(孙树祥)[1], Zhi-Chao Wei(魏志超)[2], Peng-Hui Xia(夏鹏辉)[1], Wen-Bin Wang(王文斌)[1], Zhi-Yong Duan(段智勇)[1], Yu-Xiao Li(李玉晓)[1], Ying-Hui Zhong(钟英辉)[1,†], Peng Ding(丁芃)[3], and Zhi Jin(金智)[3]

[1] *School of Physics and Engineering, Zhengzhou University, Zhengzhou* 450001, *China*
[2] *China Academy of Space Technology, Beijing* 100086, *China*
[3] *Institute of Microelectronics, Chinese Academy of Sciences, Beijing* 100029, *China*

(Received 25 September 2017; revised manuscript received 2 November 2017; published online 5 January 2018)

InP-based high electron mobility transistors (HEMTs) will be affected by protons from different directions in space radiation applications. The proton irradiation effects on InAlAs/InGaAs hetero-junction structures of InP-based HEMTs are studied at incident angles ranging from 0 to 89.9° by SRIM software. With the increase of proton incident angle, the change trend of induced vacancy defects in the InAlAs/InGaAs hetero-junction region is consistent with the vacancy energy loss trend of incident protons. Namely, they both have shown an initial increase, followed by a decrease after incident angle has reached 30°. Besides, the average range and ultimate stopping positions of incident protons shift gradually from buffer layer to hetero-junction region, and then go up to gate metal. Finally, the electrical characteristics of InP-based HEMTs are investigated after proton irradiation at different incident angles by Sentaurus-TCAD. The induced vacancy defects are considered self-consistently through solving Poisson's and current continuity equations. Consequently, the extrinsic transconductance, pinch-off voltage and channel current demonstrate the most serious degradation at the incident angle of 30°, which can be accounted for the most severe carrier sheet density reduction under this condition.

Keywords: proton irradiation, InP-based HEMTs, InAlAs/InGaAs hetero-junction, incident angle

PACS: 85.30.De, 73.61.Ey, 14.20.Dh **DOI:** 10.1088/1674-1056/27/2/028502

1. Introduction

In recent years, space exploration activities have been conducted more and more frequently and in depth, which necessarily requires all kinds of semiconductor devices and relative integrated circuits to be used in electronic systems of spacecrafts.[1,2] Among them, InP-based high electron mobility transistors (HEMTs) demonstrate extremely excellent characteristics, such as high frequency, low noise figure, superior gain performance, and so on.[3–6] Consequently, they become significantly competitive candidates for various high-speed space applications, such as national defense, aerospace, and satellite radar.[7]

Semiconductor devices and their integrated circuits have been used in harsh space environments, and they are inevitably affected by various radiation particles and rays from different directions, such as protons, electrons, neutrons, γ rays, α rays, β rays, and other secondary atomic radioactive particles,[8–10] especially, protons and electrons, which are the most abundant particles in space radiation environment. Moreover, the mass of each proton is about 1836 times heavier than that of an electron, which means more serious irradiation damage of protons. Even if radiation dose of protons may be very low, the long-time accumulated irradiation will be bound to result in performance degradation of semiconductor devices and even failure of electronic systems.

Considering high technology maturity, low fabrication cost and broad applications, research about proton irradiation effect and hardness techniques chiefly focus on Si-based complementary metal-oxide-semiconductor transistor (CMOS) and silicon-on-insulator (SOI) devices.[11,12] Admittedly, some exploratory studies have been reported to aim at proton irradiation effect on various devices with III–V materials,[13,14] and the incident direction of proton particles is almost without exception perpendicular to the device surface for both simulations and experiments. However, few studies address the effects of proton irradiation from different orientations on InP-based HEMTs, which are in accordance with actual space radiation situation.

In this paper, the proton irradiation effect on InAlAs/InGaAs hetero-junction of InP-based HEMTs is investigated by SRIM software at a proton energy of 100 keV and incident angles in a range of 0°–89.9°. On this basis, the electrical characteristics and damage mechanism of InP-based HEMTs are also analyzed under proton irradiation at different incident angles. These studies will be helpful in improving the stabilities and durabilities of relative electronic systems.

*Project supported by the National Natural Science Foundation of China (Grant Nos. 11775191, 61404115, 61434006, and 11475256), the Program for Innovative Research Team (in Science and Technology) in University of Henan Province, China (Grant No. 18IRTSTHN016), and the Development Fund for Outstanding Young Teachers in Zhengzhou University of China (Grant No. 1521317004).

†Corresponding author. E-mail: zhongyinghui@zzu.edu.cn

© 2018 Chinese Physical Society and IOP Publishing Ltd

2. Device structure

The schematic cross-section of the InP-based HEMT is shown in Fig. 1. The layers consist of an $In_{0.52}Al_{0.48}As$ buffer, an $In_{0.53}Ga_{0.47}As$ channel, an unstrained $In_{0.52}Al_{0.48}As$ spacer layer, an Si-doped plane which provides two-dimensional electron gas (2DEG), a 12-nm-thick unstrained $In_{0.52}Al_{0.48}As$ Schottky barrier layer, and a composite InGaAs cap layer composed of an Si-doped $In_{0.6}Ga_{0.4}As$ cap layer and an Si-doped $In_{0.53}Ga_{0.47}As$ transitional layer. All InAlAs layers are lattice-matched with the InP substrate.

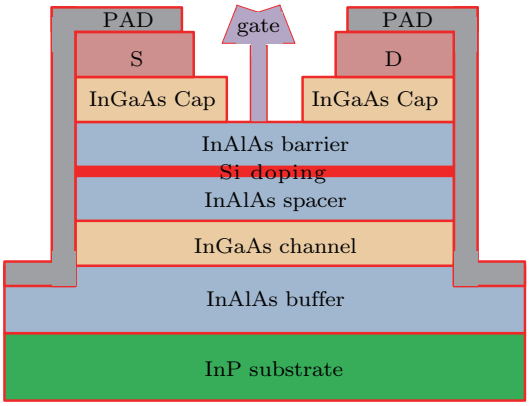


Fig. 1. (color online) The schematic cross-section of the InP-based HEMT.

As is well known, carriers are usually gathered around InAlAs/InGaAs hetero-junction in InP-based HEMT, which thus determines almost all the device characteristics, including channel current, transconductance, frequency performances, etc. Therefore, the irradiation effect of InAlAs/InGaAs hetero-junction structure can provide a theoretical basis for damage mechanism of InP-based HEMTs and even radiation-hardened scheme. The hetero-junction structure is thus intercepted from actual device,[15] which includes Ti/Pt/Au gate metals, 15-nm-thick $In_{0.52}Al_{0.48}As$ barrier and spacer layer, 15-nm-thick $In_{0.53}Ga_{0.47}As$ channel layer and 500-nm-thick $In_{0.52}Al_{0.48}As$ buffer layer as shown in Fig. 2. The III–V compound semiconductor material is treated as a series of thin layers in simulations, which is composed of respective elements with their own percentages in the compound semiconductor.

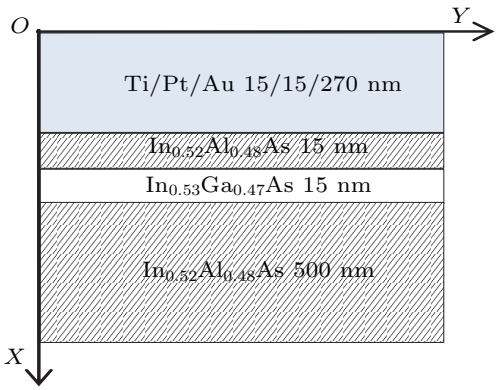


Fig. 2. (color online) Schematic structure of InAlAs/InGaAs hetero-junction.

3. Results and discussion

The damage mechanisms of proton irradiation on semiconductor devices mainly include ionization damage and displacement damage. Ionization damage mainly produces electron-hole pairs by breaking the energy band balance, and the number of the produced electron–hole pairs is proportional to the ionization energy loss (IEL) of incident protons. Displacement damage forms vacancies and replacement atoms by collision between protons and lattice atoms. Nevertheless, InP-based HEMTs have no semiconductor–insulator interfaces to capture free charges, therefore, the electron–hole pairs produced by ionization effect can be quickly recombined by diffusion motion and cannot have a permanent effect on the device characteristics. Namely, the degradation degree of device characteristics after proton irradiation is directly dependent on the number of induced vacancies by displacement effect.

The number of induced vacancy defects around InAlAs/InGaAs hetero-junction by each perpendicular incident proton is calculated by SRIM software with proton energies ranging from 40 keV to 170 keV as shown in Fig. 3. With the increase of proton energy, the proton injection depth increases gradually from metal to hetero-junction layer, therefore, the number of defects in hetero-junction region first increases and then reaches the largest value at about 80 keV. Eventually, protons pass through the material layers with only a small number of vacancies generated in the hetero-junction region. To investigate the comprehensive effects of proton irradiation on hetero-junction and device, the incident proton energy is set to be 100 keV at angles ranging from 0° to 89.9°. The maximum incident angle of 89.9° is limited by the angle range in SRIM software. Additionally, the number of incident protons is chosen to be 10^5 in the next simulations, which is large enough to make the induced vacancy defects follow the stable statistical distribution with incident depth.

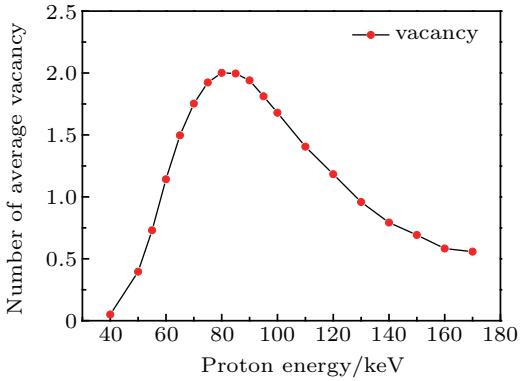


Fig. 3. (color online) Variation of induced vacancy with proton energy in InAlAs/InGaAs hetero-junction.

3.1. Irradiation damage to InAlAs/InGaAs hetero-junction at different incident angles

As illustrated above, the damage degree of the device after proton irradiation is directly related to the number of in-

duced vacancies by the displacement effect. The average number of vacancy defects generated in InAlAs/InGaAs heterojunction by each proton is obtained by integrating the vacancy density curve with respect to distance as depicted in Fig. 4(a). Meanwhile, the vacancy energy loss of each incident proton is also calculated at incident angles ranging from 0° to 89.9°, which is shown in Fig. 4(b). They both increase slightly and then decrease sharply after the incident angle has reached 30°. The same variation trend with incident angle of proton undoubtedly illustrates the principle that the number of induced vacancy defects is proportional to the vacancy energy loss of the incident proton in collision with lattice atoms.

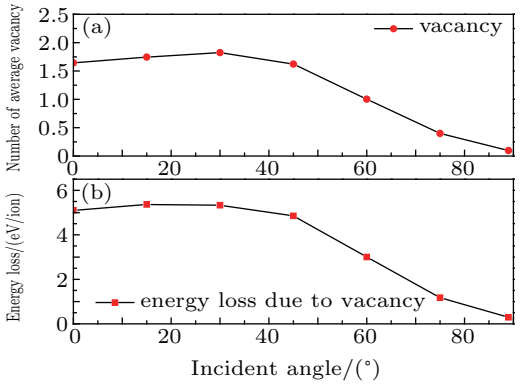


Fig. 4. (color online) Variations of (a) the number of induced vacancy defects and (b)vacancy energy loss with incident angle of proton.

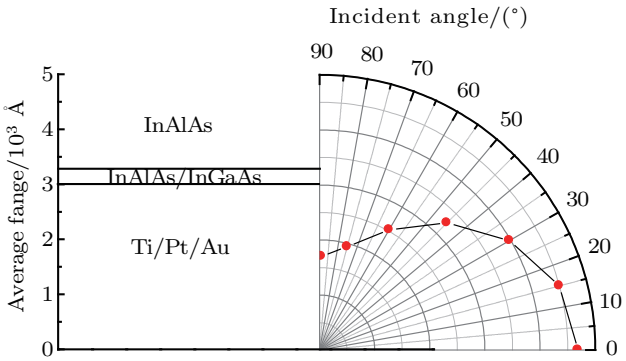


Fig. 5. (color online) Average range of protons in hetero-junction structure at different incident angles.

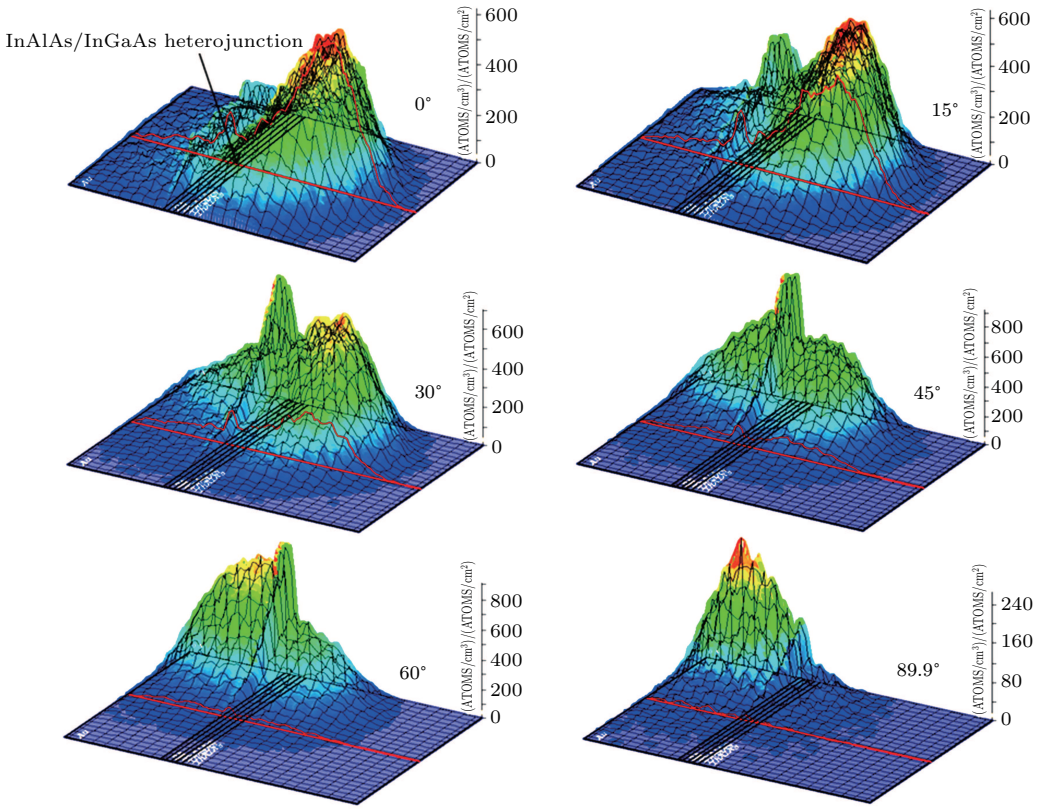


Fig. 6. (color online) Three-dimensional distributions of protons in hetero-junction structure at different incident angles.

Actually, the damage degree of hetero-junction after proton irradiation from different directions can be intuitively reflected through distribution of incident protons, that is, the damage region. The average range and ultimate stopping positions of protons in target object at different incident angles at 100 keV are shown in Figs. 5 and 6, respectively. As depicted in Fig. 5, the radius of red dots reflects the average range of protons at a given incident angle. As the proton incident angle increases from 0° to 89.9°, the red dot trajectory gradually shrinks to the center, which indicates that the average range progressively shifts from buffer layer up to gate metal. As shown in Fig. 6, the protons almost stop and distribute in hetero-junction region at an incident angle of 45°. Precisely, the stopping positions of protons would shift downward to buffer layer when incident angle is below about 45°, and transfer up to gate metal region when incident angle is

above that incident angle of 45°. Moreover, the incident protons at an incident angle of 30° will almost be distributed in buffer layer. Actually, the kinetic energy of incident protons is nearly zero at the ultimate stopping position, which will thus produce the most abundant defects before the stopping position[16] and perhaps just in hetero-junction region at an incident angle of about 30°.

3.2. Irradiation damage to InP-based HEMT at proton incident angles

As mentioned above, numerous vacancy defects are generated in InAlAs/InGaAs hetero-junction region by displacement effect after proton irradiation. The induced vacancies may influence device performances by acting as acceptor or donor defects, including As acceptor defects, In and Ga donor defects.[17] The acceptor-like defects of As vacancies behave as compensation centers of majority carriers, and thus result in performance degradation of InP-based HEMT. The induced As vacancy concentrations after proton irradiation are obtained from SRIM software at incident angles ranging from 0° to 89.9°, and the incident proton energy and fluence are set to be 100 keV and 2×10^{12} cm^{-2} in simulations. Successively, the influences of proton irradiation at different incident angles on electrical characteristics of InP-based HEMTs are investigated by Sentaurus-TCAD software. Reasonable physical models are used to describe the device performances, including hydrodynamic transport model, density gradient model, recombination models, etc. Moreover, the induced As vacancies were considered self-consistently through solving Poisson's and current continuity equations.[18]

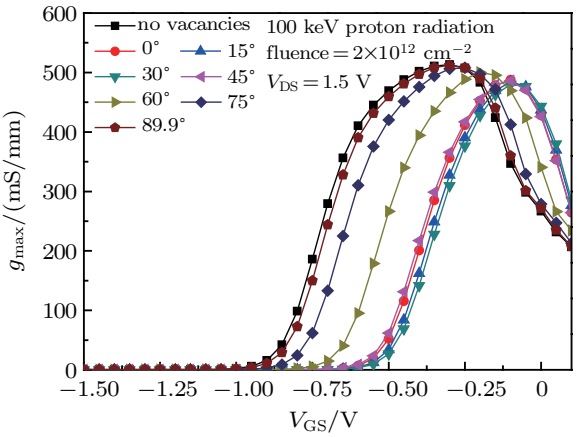


Fig. 7. (color online) Plots of extrinsic transconductance versus gate-bias voltage of InP-based HEMTs after proton irradiation at different incident angles.

Figure 7 shows the plots of extrinsic transconductance (g_m) versus gate-bias voltage (V_{GS}) of InP-based HEMTs after proton irradiation at incident angles ranging from 0° to 89.9° at a drain–source voltage (V_{DS}) of 1.5 V. The maximum values of extrinsic transconductance ($g_{m,max}$) and pinch-off voltage (V_p) after proton irradiation from different incident directions are extracted and shown in Fig. 8. With the increase of proton incident angle, V_p shifts slightly toward positive value when incident angle is below 30°, and drift gradually toward negative value when incident angle is above 30°. Besides, $g_{m,max}$ presents a decline trend till the incident angle reaches 30°, and then shows a significant increase tendency. Figure 9 shows DC current–voltage (I–V) curves for InP-based HEMTs after proton irradiation at incident angles ranging from 0° to 89.9° at a gate–source voltage (V_{GS}) of 0 V. The channel current degrades dramatically when the proton incident angle is below 30° and begins to rise up as incident angle increases. The change of device characteristics after proton irradiation from different directions can be mainly attributed to the variation of two-dimensional electron gas (2DEG) concentration in the channel region, which is greatly influenced by the induced vacancy defects in hetero-junction structure by displacement effect.[19,20]

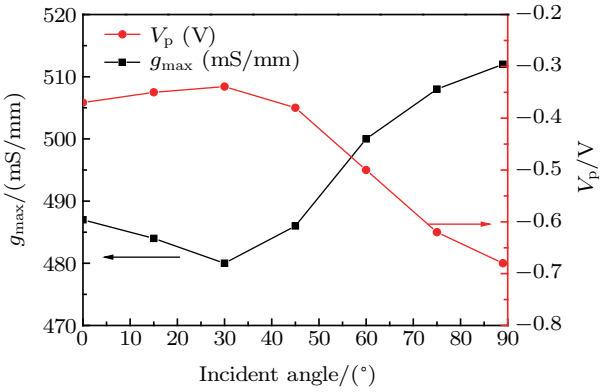


Fig. 8. (color online) Plots of maximum extrinsic transconductance and pinch-off voltage of InP-based HEMTs after proton irradiation versus incident angle.

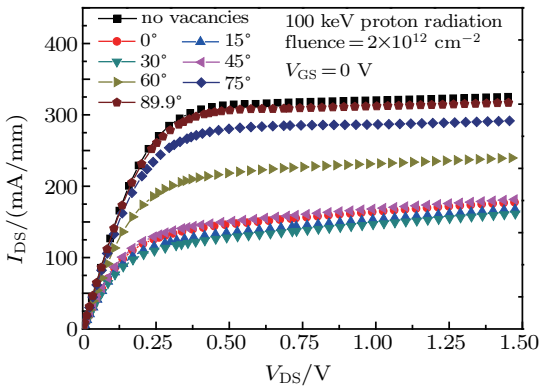


Fig. 9. (color online) I–V characteristics of InP-based HEMTs after proton irradiation at different incident angles.

The electron concentration in the channel region is investigated after proton irradiation at different incident angles, as shown in Fig. 10. As mentioned above, different numbers of As vacancies acting as acceptor defects may arise in InAlAs/InGaAs hetero-junction region after proton irradiation at different incident angles. These defects could modulate the electrical potential distribution in channel region, and shift Fermi level negatively towards the bottom of quantum well,

and thus reducing the carrier sheet density in channel region by carrier removal effect. Consequently, the transconductance performance and channel current exhibit the same variation trend with induced vacancy concentration. Meanwhile, the present acceptor-like defects would cause additional reverse modulation, which shifts the pinch-off voltage toward positive value and postpones drain-source channel current saturation.

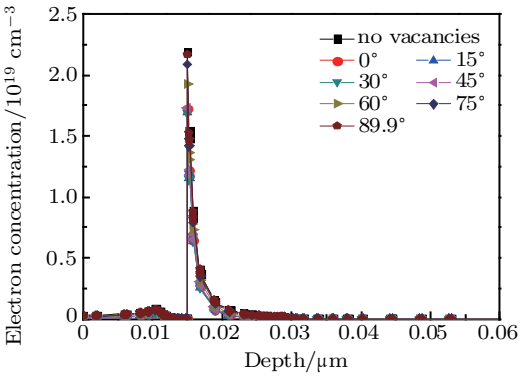


Fig. 10. (color online) Plots of electron concentration versus depth in InP-based HEMTs after proton irradiation at different incident angles.

4. Conclusions

The influences of proton irradiation from different orientations on InAlAs/InGaAs hetero-junction are studied with a proton energy of 100 keV. As the proton incident angle increases, the damage region moves gradually from buffer layer to hetero-junction region, and finally toward gate metal. Both the number of induced vacancy defects in InAlAs/InGaAs hetero-junction region and vacancy energy loss of incident protons increase slightly and then decrease sharply after the incident angle has reached 30°. Consequently, the extrinsic transconductance, pinch-off voltage and channel current demonstrate the most serious degradation at an incident angle of 30°, which can account for the most severe carrier sheet density reduction by the largest number of induced vacancy defects in InAlAs/InGaAs hetero-junction region. The above conclusions can provide a reliable theoretical guidance for assessing and reducing irradiation damage to InP-based HEMTs in space applications.

References

[1] Deal W R 2014 *The 39th International Conference on Infrared, Millimeter, and Terahertz Waves (IRMMW-THz)*, Septemmber 14–19, 2014, Tucson, AZ, USA, pp. 14–19
[2] Chen J, Puzyrev Y S, Zhang C X, Zhang E X, McCurdy M W, Fleetwood D M, Schrimpf R D, Pantelides S T, KaunS W, Kyle E C H and Speck J S 2013 *IEEE Trans. Nucl. Sci.* **60** 4080
[3] Zhong Y H, Zhang Y M, Zhang Y M, Wang X T, Lv H L, Liu X Y and Jin Z 2013 *Chin. Phys. B* **22** 128503
[4] Zhong Y H, Yang Y, Li X J, Ding P ang Jin Z 2015 *J. Korean Phys. Soc.* **66** 1020
[5] Leong K M K H, Mei X B, Yoshida W, Liu P H, Zhou Z Y, Lange M, Lee L S, Padilla J P, Zamora A, Gorospe B S, Nguyen K and Deal W R 2015 *IEEE Microwave and Wireless Components Letters* **25** 397
[6] Zhou S X, Qi M, Ai L K and Xu A H 2016 *Chin. Phys. B* **25** 096801
[7] Ajayan J and Nirmal D 2015 *Superlattices and Microstructures* **86** 1
[8] Lv L, Ma J G, Cao Y R, Zhang J C, Zhang W, Li L, Xu S R, Ma X H, Ren X T and Hao Y 2011 *Microelectronics Reliability* **51** 2168
[9] Lv L, Zhang J C, Li L, Ma X H, Cao Y R and Hao Y 2012 *Acta Phys. Sin.* **61** 057202 (in Chinese)
[10] Gu W P, Zhang L, Li Q H, Qiu Y Z, Hao Y, Quan S and Liu P Z 2014 *Acta Phys. Sin.* **63** 047202 (in Chinese)
[11] Carniti P, Cassina L, Gotti C, Maino C and Pessina G 2016 *Nucl. Instrum. Methods Phys. Res. A* **824** 258
[12] Kurachi I, Kobayashi K, Okihara M, Kasai H, Hatsui T, Hara K, Miyoshi T and Arai Y 2015 *IEEE Trans. Electron Dev.* **62** 2371
[13] Tunhuma S M, Auret F D, Legodi M J and Diale M 2016 *J. Appl. Phys.* **119** 145705
[14] Anderson T J, Koehler A D, Greenlee J D, Weaver B D, Mastro A M, Hite J K, Eddy C R, Kub F J and Hobart K D 2014 *IEEE Electron Dev. Lett.* **35** 826
[15] Zhong Y H, Wang X T, Su Y B, Cao Y X, Jin Z, Zhang Y M and Liu X Y 2012 *J. Semicond.* **33** 43
[16] Xue J X, Zhang G J, Guo L P, Zhang H B, Wang X G, Zou J, Peng S M and Long X H 2014 *J. European Ceram. Soc.* **34** 633
[17] Liu M, Zhang Y M, Lu H L, Zhang Y M, Zhang J C and Ren X T 2015 *Solid-State Electron.* **109** 52
[18] Patrick E E, Choudhury M, Ren F, Pearton S J and Law M E 2015 *ECS J. Solid State Sci. Technol.* **4** Q21
[19] Movlaa H, Babazadeha M and Sadreddini S V 2016 *Optik* **127** 3844
[20] Yannakopoulos P H, Skountzos A P and Veselyb M 2008 *Microelectronics Journal* **39** 732